Pnicogen bonded complexes of PO2X (X = F, Cl) with nitrogen bases

ARTICLE *in* THE JOURNAL OF PHYSICAL CHEMISTRY A · SEPTEMBER 2013

Impact Factor: 2.69 · DOI: 10.1021/jp407097e · Source: PubMed

3 AUTHORS, INCLUDING:

Ibon Alkorta
Spanish National Research Council
679 PUBLICATIONS **12,371** CITATIONS
SEE PROFILE

José Elguero
Spanish National Research Council
1,502 PUBLICATIONS **22,122** CITATIONS
SEE PROFILE

THE JOURNAL OF PHYSICAL CHEMISTRY A

Article

pubs.acs.org/JPCA

Pnicogen Bonded Complexes of PO_2X (X = F, Cl) with Nitrogen Bases

Ibon Alkorta* and José Elguero

Instituto de Química Médica (IQM-CSIC), Juan de la Cierva, 3, 28006 Madrid, Spain

Janet E. Del Bene*

Department of Chemistry, Youngstown State University, Youngstown, Ohio 44555, United States

Supporting Information

ABSTRACT: An ab initio MP2/aug′-cc-pVTZ study has been carried out on complexes formed between PO_2X (X = F and Cl) as the Lewis acids and a series of nitrogen bases ZN, including NH_3, $H_2C{=}NH$, NH_2F, NP, NCH, NCF, NF_3, and N_2. Binding energies of these complexes vary from −10 to −150 kJ/mol, and P—N distances from 1.88 to 2.72 Å. Complexes ZN:PO_2F have stronger P···N bonds and shorter P—N distances than the corresponding complexes ZN:PO_2Cl. Charge transfer from the N lone pair through the π-hole to the P—X and P—O σ^* orbitals leads to stabilization of these complexes, although charge-transfer energies can be evaluated only for complexes with binding energies less than −71 kJ/mol. Complexation of PO_2X with the strongest bases leads to P···N bonds with a significant degree of covalency, and P—N distances that approach the P—N distances in the molecules PO_2NC and PO_2NH_2. In these complexes, the PO_2X molecules distort from planarity. Changes in ^{31}P absolute chemical shieldings upon complexation do not correlate with changes in charges on P, although they do correlate with the binding energies of the complexes. EOM-CCSD spin−spin coupling constants ^{1p}J(P—N) are dominated by the Fermi-contact term, which is an excellent approximation to total J. ^{1p}J(P—N) values are small at long distances, increase as the distance decreases, but then decrease at short P—N distances. At the shortest distances, values of ^{1p}J(P—N) approach ^{1}J(P—N) for the molecules PO_2NC and PO_2NH_2.

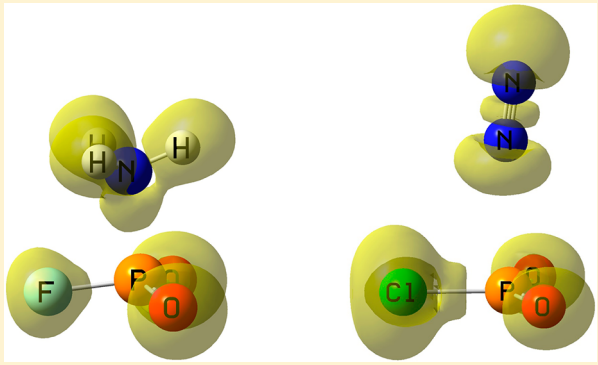

INTRODUCTION

The pnicogen bond is a Lewis acid−Lewis base attractive interaction in which a pnicogen atom (N, P, or As) is the Lewis acid. Although complexes with pnicogen bonds have been known for some time,[1−6] it was subsequent to the landmark paper by Hey-Hawking et al.[7] in 2011 that this interaction became the subject of intense investigation. This is evident from the papers on pnicogen bonding published since then.[8−35]

The electrostatic component of the pnicogen bond has been described in terms of the σ-hole concept proposed by Politzer and Murray.[5] The term σ-hole refers to the electron-deficient outer lobe of a p orbital of an electronegative atom that is involved in bond formation as an electron-pair acceptor. In addition, there can also exist a π-hole, a positive region of the molecular electrostatic potential that is perpendicular to an adjacent portion of the molecular framework.[36] Diederich et al. coined the term "orthogonal interaction" for interactions in which an electron donor interacts with a π-hole.[37] Charge transfer, which also plays a significant role in the stabilization of complexes with pnicogen bonds, may involve electron donation through a σ-hole or a π-hole. For a given base, which mechanism is active depends on the nature of the pnicogen-containing molecule.

Our previous studies of pnicogen bonds have focused exclusively on those involving σ-holes.[20,21,25−28,31−33,35] To examine pnicogen complexes formed through π-holes, we have attached very electronegative substituents to a phosphorus atom to form the Lewis acids PO_2F and PO_2Cl, and have examined the complexes formed by these acids with a series of electron-donating nitrogen bases ZN, including NH_3, $H_2C{=}NH$, NH_2F, NP, NCH, NCF, NF_3, and N_2. In this paper we present the structures and binding energies of complexes ZN:PO_2X, their bonding and electronic properties, and the NMR properties of ^{31}P absolute chemical shieldings and ^{31}P—^{15}N spin−spin coupling constants.

COMPUTATIONAL METHODS

The structures of the isolated monomers and complexes were optimized at second-order Møller−Plesset perturbation theory (MP2)[38−41] with the aug′-cc-pVTZ basis set.[42] This basis set is derived from the Dunning aug-cc-pVTZ basis set[43,44] by removing diffuse functions from H atoms. Frequencies were

Received: July 17, 2013
Revised: August 25, 2013
Published: September 17, 2013

   dx.doi.org/10.1021/jp407097e | J. Phys. Chem. A 2013, 117, 10497−10503

computed to establish that the optimized structures correspond to equilibrium structures on their potential surfaces. Optimization and frequency calculations were performed using the Gaussian09 program.[45]

The electron densities of the complexes have been analyzed using the Atoms in Molecules (AIM) methodology[46−49] and the Electron Localization Function (ELF),[50] employing the AIMAll[51] and Topmod[52] programs. The topological analysis of the electron density produces the molecular graph of each complex. This graph identifies the location of electron density features of interest, including the electron density (ρ) maxima associated with the various nuclei, saddle points which corresponds to bond critical points (BCPs), and ring critical points which indicate a minimum electron density within a ring. The zero gradient line that connects a BCP with two nuclei is the bond path. The electron density at the BCP (ρ_{BCP}), the Laplacian of the electron density at the BCP ($\nabla^2\rho_{BCP}$), and the total energy density (H_{BCP}) are additional useful quantities for characterizing interactions.[53] The ELF function illustrates those regions of space at which the electron density is high. Using all of these measures, it is easy to identify bonds and lone pairs, and to characterize bond types

The Natural Bond Orbital (NBO) method[54] has been used to obtain atomic charges and to analyze the stabilizing charge-transfer interactions in these binary complexes. The NBO-5 program[55] within the Gamess program[56] has been used for the NBO calculations. The molecular electrostatic potentials (MEPs) of the isolated PO_2X monomers have been calculated with the Gaussian09 program. These have been represented on the 0.001 au electron density isosurfaces using the WFA program.[57]

Absolute chemical shieldings have been calculated for all complexes at MP2/aug′-cc-pVTZ using the GIAO approximation.[58] Spin−spin coupling constants were evaluated using the equation-of-motion coupled cluster singles and doubles (EOM-CCSD) method in the CI (configuration interaction)-like approximation,[59,60] with all electrons correlated. For these calculations, the Ahlrichs[61] qzp basis set was placed on ^{13}C, ^{15}N, ^{17}O, and ^{19}F, and the qz2p basis set on ^{31}P and ^{35}Cl. The Dunning cc-pVDZ basis set was placed on all H atoms. Paramagnetic spin−orbit (PSO), diamagnetic spin−orbit (DSO), Fermi-contact (FC), and spin dipole (SD) contributions to the total coupling constant have been evaluated for all complexes except $F_3N:PO_2Cl$, in which case J has been approximated by the FC term. Only ^{1p}J(P—P) coupling constants are reported in this paper. The EOM-CCSD calculations were performed using ACES II[62] on the IBM Cluster 1350 (Glenn) at the Ohio Supercomputer Center.

RESULTS AND DISCUSSION

PO_2X Monomers. The isolated PO_2X molecules have C_{2v} symmetry. Available experimental structural data for PO_2Cl[63] are reported in Table 1. Corresponding computed values are given for both PO_2Cl and PO_2F. There is reasonably good agreement between the computed and the experimental structure of PO_2Cl, although the computed P═O and P—Cl bond lengths overestimate the experimental values by about 0.02 Å.

The molecular electrostatic potentials on the 0.001 au electron density isosurfaces of PO_2F and PO_2Cl are illustrated in Figure 1. The MEPs are very negative around the oxygen atoms, slightly negative around the halogen atoms, and positive above and below the phosphorus atoms. These positive regions correspond to the π-holes. The MEP values at the π-holes are 0.099 and 0.078 au for PO_2F and PO_2Cl, respectively. The MEPs of these molecules resemble the MEPs of halogenated nitryl derivatives.[64]

Table 1. Experimental and Calculated PO_2X Bond Distances (Å) and Bond Angles (deg)

	PO_2F	PO_2Cl	
parameter	calc	exp[a]	calc
P═O	1.467	1.448	1.471
P—Cl/F	1.554	1.972	1.992
O═P═O	135.9	134.2	134.6

[a]Reference 63.

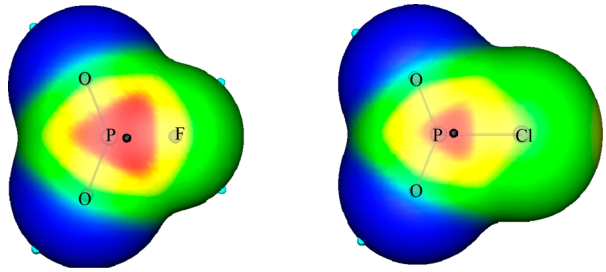

Figure 1. MEPs on the 0.001 au electron density surfaces of PO_2F and PO_2Cl. The positions of the maximum and minima on each surface are represented by black and light blue dots, respectively. Color code scale (au): red > 0.06 > yellow > 0.03 > green > 0.0 > blue.

Geometries and Energies of Complexes ZN:PO_2X. The geometries and energies of complexes ZN:PO_2X are reported in Table S1 of the Supporting Information. Interaction energies and intermolecular P—N distances are given in Table 2. The interaction energies range from −13 to −148 kJ/mol. P—N distances in these same complexes vary between 1.88 and 2.90 Å. The shortest distances in each series are found in the complexes having H_2C═NH as the base, followed by NH_3; the longest distances occur in complexes with N_2. Based on Table 2, it is possible to subdivide these complexes into three groups. One group includes complexes formed with the strongest bases, NH_3, H_2C═NH, and NH_2F. These complexes are found at P—N distances between 1.878 and 1.962 Å and have interaction energies between −90.2 and −148.5 kJ/mol. The second group of complexes contains the sp hybridized nitrogen bases PN, HCN, and FCN, have P—N distances between 1.926 and 2.295 Å, and have binding energies between −36.7 and −87.4 kJ/mol. Note that there is an overlap between the P—N distances of PN:PO_2F, the most strongly bound complex

Table 2. Interaction Energies (ΔE, kJ/mol) and P—N Distances (R, Å) in Complexes ZN:PO_2X

	PO_2F		PO_2Cl	
	ΔE	R	ΔE	R
$H_3N:PO_2X$	−148.49	1.902	−128.55	1.912
H_2C═(H)N:PO_2X	−146.19	1.878	−126.00	1.893
$H_2FN:PO_2X$	−105.10	1.953	−90.15	1.962
$PN:PO_2X$	−87.43	1.926	−70.26	1.949
$HCN:PO_2X$	−60.37	2.042	−42.80	2.161
$FCN:PO_2X$	−52.04	2.096	−36.74	2.295
$F_3N:PO_2X$	−21.78	2.381	−16.50	2.646
$N_2:PO_2X$	−15.39	2.725	−12.85	2.897

dx.doi.org/10.1021/jp407097e | J. Phys. Chem. A 2013, 117, 10497−10503

in the second group, and $H_2FN{:}PO_2Cl$, the weakest in the first. The third group is made up of complexes with the weak bases NF_3 and N_2. These have binding energies between −12.5 and −21.8 kJ/mol, and P—N distances between 2.381 and 2.897 Å. These groupings are consistent with the proton affinities listed in the NIST database:[65] NH_3 (853.6) > $H_2C{=}NH$ (818.7) > NP (789.4) > NCH (712.9) > NF_3 (568.4) > N_2 (493.8). From Table 2 it can also be seen that the interaction energy is greater and the P—N distance shorter in $ZN{:}PO_2F$ than in the corresponding complex $ZN{:}PO_2Cl$. Figure 2 presents a plot of the binding energies of these complexes versus the P—N distance.

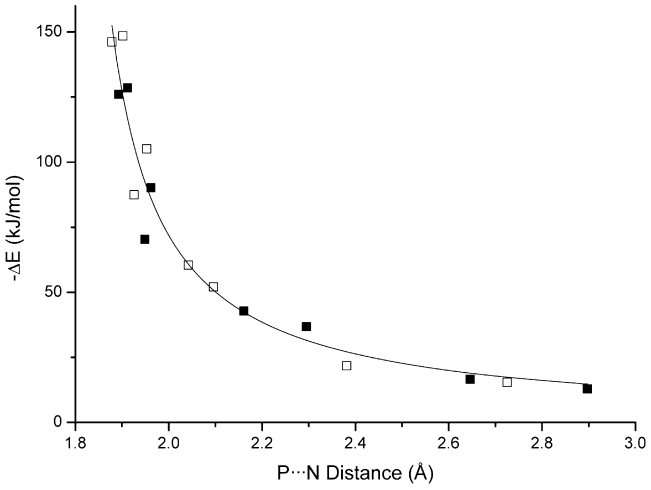

Figure 2. Negative of the interaction energy $(-\Delta E)$ versus the P—N distance. Empty and solid squares correspond to the PO_2F and PO_2Cl complexes, respectively. The best-fit trendline has the form $-\Delta E = 1/[a + bR(\text{P—N})]$, and a correlation coefficient $R^2 = 0.94$.

There are two other interesting structural features of these complexes. The first is the distortion of the PO_2X molecules upon complexation with the stronger nitrogen bases. The degree of distortion from planarity can be measured as the sum of the bond angles around P, which is 360° for a planar structure and 328.4° for a tetrahedral structure. When the base is $H_2C{=}NH$, this sum is 351.7° and 352.2° for PO_2Cl and PO_2F, respectively; for N_2, it is 360.0° and 359.9°, respectively. It is also important to note that the short P—N distances in the complexes with the strongest bases are approaching the P—N distances of the covalent P—N bonds in the molecules PO_2NH_2 and PO_2NC. The computed MP2/aug′-cc-pVTZ P—N distances in these molecules are 1.63 and 1.67 Å, respectively.

Electronic Properties of Complexes $ZN{:}PO_2X$. The molecular graphs of complexes $ZN{:}PO_2F$ and $ZN{:}PO_2Cl$ are shown in Table S1 of the Supporting Information. The ELF representations illustrated in Figure 3 for the most strongly bound complex $H_3N{:}PO_2F$, and for the weakest, $N_2{:}PO_2Cl$, clearly illustrate lone pair donation by the nitrogen base and acceptance through the π-hole of phosphorus. Consistent with this picture, the AIM analysis of the electron density shows the presence of one intermolecular bond critical point (BCP) and a corresponding bond path connecting the phosphorus atom of the PO_2X molecule with the nitrogen atom of the base. The electron densities at the BCPs range from 0.013 to 0.159 au, and are exponentially related to the intermolecular P—N distances, with a correlation coefficient R^2 of 0.994, in

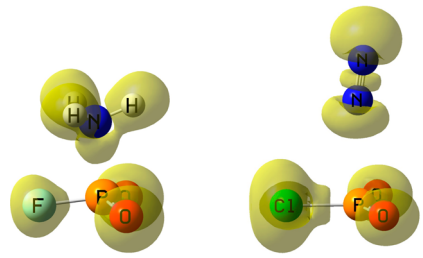

Figure 3. ELF 0.75 au isosurfaces of $H_3N{:}PO_2F$ and $N_2{:}PO_2Cl$ illustrating the interaction between the lone pair on N and the π-hole on P.

agreement with previous studies of weak interactions.[66−74] The Laplacian at the BCP is always positive, with values between 0.017 and 0.347 au. In contrast, the total energy density H is negative except for the four most weakly bound complexes with the bases NF_3 and N_2. The relatively large negative values of H are a clear indication of the covalent character of the stronger P···N bonds.

The delocalization index (DI)[75] is a computed index that measures the number of electron pairs delocalized between two atoms. The DI values for the phosphorus and nitrogen atoms in complexes $ZN{:}PO_2X$ range from 0.04 to 0.29 e. The plots in Figure 4 of the DI versus the intermolecular P—N distance for each series show excellent exponential correlations.

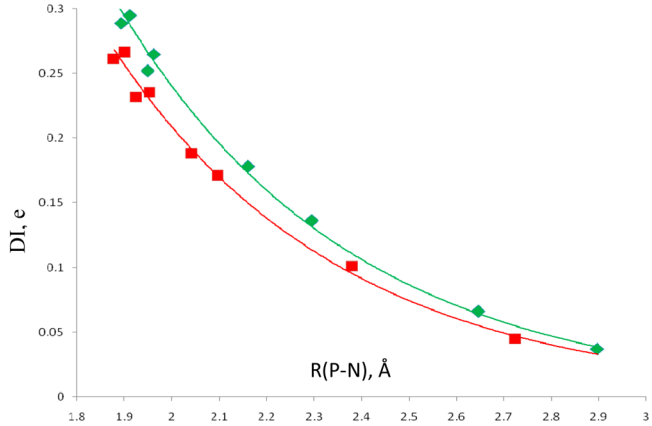

Figure 4. P···N delocalization index (DI) vs the intermolecular P—N distance. The exponential trendlines have correlation coefficients R^2 greater than 0.99.

The NBO method has been used to evaluate the stabilizing intermolecular charge-transfer interaction energies, which are reported in Table 3. The evaluation of charge-transfer energies is only possible for complexes with binding energies less than −71 kJ/mol, because the NBO method treats complexes with greater binding energies as single molecules, thereby producing unrealistic charge-transfer energy values. In the more weakly bound complexes, charge transfer occurs from the nitrogen lone pair to the antibonding σ^* P—O and P—X orbitals through the π-hole. As a result, PO_2X gains electron density and becomes negatively charged, while the nitrogen base loses electron density and becomes positively charged. The amount of charge transfer can be as large as 0.30 e, which is only slightly less than the 0.37 e charge transfer computed for the prototypical complex $H_3B{:}NH_3$ with a dative bond. Not surprisingly, the computed NBO bond orders in each series follow essentially the same pattern as the degree of charge

dx.doi.org/10.1021/jp407097e | J. Phys. Chem. A 2013, 117, 10497−10503

Table 3. Total Charge Transfer (e), Second-Order Charge-Transfer Stabilization Energies [N(lp) → σ*(P—Y), kJ/mol], and N···P Bond orders

	total charge transfer		total N(lp) → σ*(P—Y)[a]		N···P bond order	
complex	X = F	X = Cl	X = F	X = Cl	X = F	X = Cl
$H_3N{:}PO_2X$	0.286	0.296	*b*	*b*	0.43	0.43
$H_2CHN{:}PO_2X$	0.245	0.251	*b*	*b*	0.44	0.44
$FH_2N{:}PO_2X$	0.246	0.244	*b*	*b*	0.37	0.38
$PN{:}PO_2X$	0.127	0.127	*b*	321.3	0.37	0.37
$HCN{:}PO_2X$	0.130	0.107	219.2	159.8	0.27	0.21
$FCN{:}PO_2X$	0.117	0.077	188.3	96.4	0.23	0.15
$F_3N{:}PO_2X$	0.079	0.043	69.5	32.8	0.11	0.06
$N_2{:}PO_2X$	0.013	0.008	19.0	12.6	0.03	0.02

[a]P—Y includes the P—X and the two P—O bonds. [b]The NBO method treats these complexes as molecules with an intramolecular P—N bond.

transfer, the binding energies, and the intermolecular distances. Thus, the bond orders range from 0.02 and 0.03 for $N_2{:}PO_2Cl$ and $N_2{:}PO_2F$, respectively, to 0.44 for complexes with $H_2C{=}$NH. An exponential relationship with a correlation coefficient R^2 of 0.992 exists between the bond order and the P—N distance.

Chemical Shieldings. Absolute chemical shieldings and charges on P in the isolated monomers PO_2F and PO_2Cl, and the changes in these quantities upon complex formation, are reported in Table 4. Complexation produces an increase in ^{31}P

Table 4. Changes in ^{31}P Absolute Chemical Shieldings (Δσ, ppm) and NBO Charges on P (Δe, au) upon Formation of Complexes $ZN{:}PO_2X$

	X = F		X = Cl	
	$\Delta\sigma(^{31}P)$[a]	Δe[b]	$\Delta\sigma(^{31}P)$[a]	Δe[b]
$H_3N{:}PO_2X$	58.79	0.030	76.76	0.032
$H_2CHN{:}PO_2X$	58.33	0.036	70.88	0.034
$FH_2N{:}PO_2X$	50.29	0.011	67.79	0.062
$PN{:}PO_2X$	46.83	0.061	58.33	−0.035
$HCN{:}PO_2X$	37.72	0.057	33.21	0.026
$FCN{:}PO_2X$	31.32	0.056	19.07	0.061
$F_3N{:}PO_2X$	10.62	0.009	2.37	0.007
$N_2{:}PO_2X$	2.47	0.022	0.08	−0.027

[a]Monomer $\sigma(^{31}P)$ values: PO_2F = 318.0 ppm; PO_2Cl = 293.5 ppm. [b]Monomer P charges: PO_2F = 2.42 e; PO_2Cl = 2.10 e.

chemical shieldings, varying from 2 to 59 ppm in complexes with PO_2F, and from 0.1 to 77 ppm in those with PO_2Cl. As evident from Table 4, the change in chemical shieldings does not correlate with the change in the charges on P, an observation made previously for other pnicogen bonded complexes.[27,31−35] However, the increase in the chemical shieldings of complexes in each series does correlate with the interaction energies of these complexes, as illustrated in Figure 5.

Coupling Constants. $^{31}P—^{31}P$ spin−spin coupling constants across intermolecular pnicogen bonds in complexes $ZN{:}PO_2F$ and $ZN{:}PO_2Cl$ are reported in Table 5. As observed previously, the Fermi-contact (FC) term is an excellent approximation to total $^{1p}J(P—P)$. The largest difference between the FC term and total *J* is less than 2 Hz in complexes with NH_3, and no more than 1 Hz in the remaining complexes.

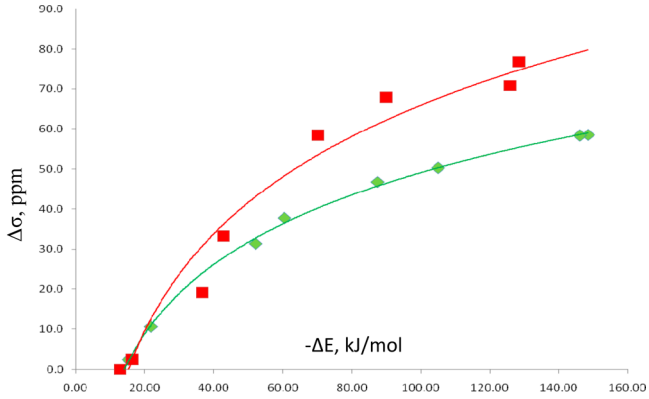

Figure 5. Changes in the ^{31}P chemical shieldings (Δσ) upon complexation vs the negative of the interaction energies (−Δ*E*) of complexes $ZN{:}PO_2F$ (◆) and $ZN{:}PO_2Cl$ (■). The logarithmic trendlines have correlation coefficients R^2 of 0.998 and 0.963 for $ZN{:}PO_2F$ and $ZN{:}PO_2Cl$, respectively.

Table 5. Spin−Spin Coupling Constants $^{1p}J(P—N)$ and Their Components (Hz) for Complexes $ZN{:}PO_2F$ and $ZN{:}PO_2Cl$ and Molecules PO_2NH_2 and PO_2NC

$ZN{:}PO_2F$	PSO	DSO	FC	SD	$^{1p}J(P—N)$
$ZN{=}NH_3$	0.0	−0.1	21.6	−1.4	20.1
$NHCH_2$	0.5	−0.2	17.6	−1.0	17.0
NH_2F	0.3	−0.2	30.1	−1.1	29.1
NP	0.9	−0.2	48.2	−0.3	48.7
NCH	0.2	−0.1	57.7	−0.2	57.6
NCF	0.1	−0.1	64.4	−0.1	64.2
NF_3	0.1	−0.2	40.0	0.0	39.9
N_2	0.0	−0.1	12.3	0.0	12.2
$ZN{:}PO_2Cl$	PSO	DSO	FC	SD	$^{1p}J(P—N)$
$ZN{=}NH_3$	−0.2	−0.1	30.2	−1.5	28.4
$NHCH_2$	0.4	−0.2	30.7	−0.9	30.0
NH_2F	0.3	−0.2	39.6	−1.2	38.6
NP	0.8	−0.2	64.4	−0.3	64.7
NCH	0.0	−0.1	65.5	−0.1	65.3
NCF	−0.1	−0.1	54.8	0.0	54.6
NF_3[a]			18.8		
N_2	0.0	−0.1	5.7	0.0	5.6
molecule	PSO	DSO	FC	SD	$^{1}J(P—N)$
PO_2NC	4.6	−0.1	−4.0	−0.7	−0.3
PO_2NH_2	9.9	−0.1	−36.1	−0.3	−26.6

[a]Because of the computational cost, only the FC term has been computed for $F_3N{:}PO_2Cl$.

Figure 6 presents plots of $^{1p}J(P—N)$ versus the P—N distance for complexes $ZN{:}PO_2F$ and $ZN{:}PO_2Cl$. These plots indicate that at long distances $^{1p}J(P—N)$ values are relatively small, increase to a maximum, and then decrease as the P—N distance decreases. The points for each trendline can be grouped in a similar way to the groupings used for distances and binding energies. At long distances with relatively small $^{1p}J(P—N)$ values are the complexes with the weakest bases NF_3 and N_2. Coupling constants for these bases vary from 6 to 40 Hz. As the P—N distance continues to decrease, the coupling constants in the second group consisting of the sp hybridized bases NP, NCH, and NCF increase and vary between 49 and 65 Hz. As the P—N distance decreases further, $^{1p}J(P—N)$ also decreases for complexes with the strongest bases NH_3, $HN{=}CH_2$, and NH_2F, varying between 17 and 39 Hz. Although the

dx.doi.org/10.1021/jp407097e | J. Phys. Chem. A 2013, 117, 10497−10503

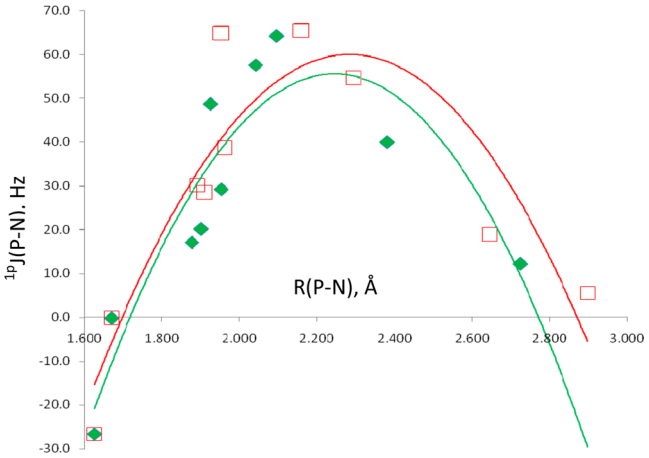

Figure 6. ^{1p}J(P—N) versus R(P—N) for complexes ZN:PO_2F (◆) and ZN:PO_2Cl (□). The points for PO_2NH_2 and PO_2NC have been included with both series. The correlation coefficients R^2 are 0.84 and 0.83, respectively.

correlation coefficients of the trendlines are not good, the trendlines do provide a clear indication of coupling-constant patterns. For complexes ZN:PO_2F and ZN:PO_2Cl, ^{1p}J(P—N) values are not useful for estimating P—N distances, because two different distances can have the same value of ^{1p}J(P—N).

As noted above, the short distances in the complexes with NH_3, $H_2C{=}NH$, and NH_2F approach the P—N distances found in the molecules PO_2NC and PO_2NH_2, and ^{1p}J(P—N) values in these complexes approach the values of ^1J(P—N) in the molecules. The plots in Figure 6 include the points for these two molecules, and the trendlines include the values of −0.3 and −26.6 Hz, respectively. Similar behavior has been observed previously for complexes nFH:$(PH_2F)_2$ and nFH:$(H_2FP{:}NFH_2)_2$ when all FH are hydrogen bonded to the same P—F bond, and in complexes LA:$H_2FP{:}NFH_2$ and LA:$H_3P{:}NH_3$ in which P also acts as an electron-pair donor to a Lewis acid.[27,28,33] Finally, it is important to note once again that although the FC term is a very good approximation to ^{1p}J(P—N) for coupling across the intermolecular pnicogen bond, it is not a good approximation for ^1J(P—N) in molecules. Relative to the complexes, the FC terms in the molecules change sign, and the PSO terms assume increased importance.

CONCLUSIONS

Ab initio MP2/aug′-cc-pVTZ calculations have been performed on a series of complexes with PO_2F and PO_2Cl as the Lewis acids and the nitrogen bases NH_3, $H_2C{=}NH$, NH_2F, NP, NCH, NCF, NF_3, and N_2 as the electron donors. These calculations support the following statements.

1. On the basis of their P—N distances and binding energies, these complexes can be subdivided into three groups: those involving the strong bases NH_3, $H_2C{=}NH$, NH_2F; those with the intermediate strength sp hybridized bases NP, NCH, NCF; and those with the weak bases NF_3 and N_2. The first group has the highest binding energies and shortest P—N distances, whereas the last group has the weakest binding energies and longest P—N distances. Complexes ZN:PO_2F have stronger P···N bonds and shorter P—N distances than the corresponding complexes ZN:PO_2Cl.
2. Charge transfer from the N lone pair through the π-hole to the σ^* P—X and P—O orbitals leads to stabilization of these complexes, although charge-transfer energies can be evaluated only for complexes with binding energies less than −71 kJ/mol. Complexation of PO_2X with the strongest bases leads to P···N bonds with a significant degree of covalency, and P—N distances that approach the P—N distances in the molecules PO_2NC and PO_2NH_2. In these complexes, the PO_2X molecules distort from planarity.
3. Changes in ^{31}P absolute chemical shieldings upon complexation do not correlate with the changes in the charges on P. However, they do correlate with the binding energies of the complexes.
4. EOM-CCSD spin−spin coupling constants ^{1p}J(P—N) are dominated by the Fermi-contact terms, which are excellent approximations to total J. As a function of the P−N distance, ^{1p}J(P—N) values are small at long distance, increase as the distance decreases, but then decrease at short P—N distances. At the shortest distances, values of ^{1p}J(P—N) approach ^1J(P—N) for the molecules PO_2NC and PO_2NH_2.

ASSOCIATED CONTENT

Supporting Information

Molecular graphs, geometries, and energies of complexes ZN:PO_2F and ZN:PO_2Cl; full refs 45, 56, and 62. This material is available free of charge via the Internet at http://pubs.acs.org.

AUTHOR INFORMATION

Corresponding Authors

*I. Alkorta: e-mail, ibon@iqm.csic.es.
*J. E. Del Bene: e-mail, jedelbene@ysu.edu.

Notes

The authors declare no competing financial interest.

ACKNOWLEDGMENTS

This work was carried out with financial support from the Ministerio de Economía y Competitividad (Project No. CTQ2012-35513-C02-02) and Comunidad Autónoma de Madrid (Project MADRISOLAR2, ref S2009/PPQ1533). Thanks are also given to the Ohio Supercomputer Center and CTI (CSIC) for their continued support.

REFERENCES

(1) Widhalm, M.; Kratky, C. Synthesis and X-ray Structure of Binaphthyl-Based Macrocyclic Diphosphanes and their Ni(II) and Pd(II) Complexes. *Chem. Ber.* **1992**, *125*, 679−689.
(2) Drago, R. S.; Wong, N.; Ferris, D. C. The E, C, T Interpretation of Bond Dissociation Energies and Anion-Neutral Molecule Interactions. *J. Am. Chem. Soc.* **1991**, *113*, 1970−1977.
(3) Carré, F.; Chuit, C.; Corriu, R. J. P.; Mongorte, P.; Nayyar, N. K.; Reyé, C. Intramolecular Coordination at Phosphorus: Donor-Acceptor Interaction in Three- and Four-Coordinated Phosphorus Compounds. *J. Organomet. Chem.* **1995**, *499*, 147−154.
(4) Klinkhammer, K. W.; Pyykko, P. Ab Initio Interpretation of the Closed-Shell Intermolecular E···E Attraction in Dipnicogen ($H_2E{-}EH_2$)$_2$ and Dichalcogen (HE-EH)$_2$ Hydride Model Dimers. *Inorg. Chem.* **1995**, *34*, 4134−4138.
(5) Murray, J. S.; Lane, P.; Politzer, P. A Predicted New Type of Directional Noncovalent Interaction. *Int. J. Quantum Chem.* **2007**, *107*, 2286−2292.

(6) Mohajeri, A.; Pakirai, A. H.; Bagheri, N. Theoretical Studies on the Nature of Bonding in σ-Hole Complexes. *Chem. Phys. Lett.* **2009**, *467*, 393−397.
(7) Zahn, S.; Frank, R.; Hey-Hawkins, E.; Kirchner, B. Pnicogen Bonds: A New Molecular Linker? *Chem.—Eur. J.* **2011**, *17*, 6034−6038.
(8) Solimannejad, M.; Gharabaghi, M.; Scheiner, S. SH···N and SH···P Blue-Shifting H-Bonds and N···P Interactions in Complexes Pairing HSN with Amines and Phosphines. *J. Chem. Phys.* **2011**, *134* (024312), 1−6.
(9) Scheiner, S. A New Noncovalent Force: Comparison of P ···N Interaction with Hydrogen and Halogen Bonds. *J. Chem. Phys.* **2011**, *134* (094315), 1−9.
(10) Scheiner, S. Effects of Substituents upon the P···N Noncovalent Interaction: The Limits of its Strength. *J. Phys. Chem. A* **2011**, *115*, 11202−11209.
(11) Politzer, P.; Murray, J. Halogen Bonding and Beyond: Factors Influencing the Nature of CN−R and SiN−R Complexes with F−Cl and Cl_2. *Theor. Chem. Acc.* **2012**, *131* (1114), 1−10.
(12) Adhikari, U.; Scheiner, S. Substituent Effects on Cl···N, S···N, and P···N Noncovalent Bonds. *J. Phys. Chem. A* **2012**, *116*, 3487−3497.
(13) Adhikari, U.; Scheiner, S. Sensitivity of Pnicogen, Chalcogen, Halogen and H-Bonds to Angular Distortions. *Chem. Phys. Lett.* **2012**, *532*, 31−35.
(14) Scheiner, S. Can Two Trivalent N Atoms Engage in a Direct N N Noncovalent Interaction? *Chem. Phys. Lett.* **2011**, *514*, 32−35.
(15) Scheiner, S. Effects of Multiple Substitution upon the P···N Noncovalent Interaction. *Chem. Phys.* **2011**, *387*, 79−84.
(16) Scheiner, S. On the Properties of X···N Noncovalent Interactions for First-, Second-, and Third-Row X Atoms. *J. Chem. Phys.* **2011**, *134* (164313), 1−9.
(17) Adhikari, U.; Scheiner, S. Comparison of P···D (D = P, N) with other Noncovalent Bonds in Molecular Aggregates. *J. Chem. Phys.* **2011**, *135* (184306), 1−10.
(18) Scheiner, S.; Adhikari, U. Abilities of Different Electron Donors (D) to Engage in a P···D Noncovalent Interaction. *J. Phys. Chem. A* **2011**, *115*, 11101−11110.
(19) Scheiner, S. Weak H-Bonds. Comparisons of CHO to NHO in Proteins and PHN to Direct PN Interactions. *Phys. Chem. Chem. Phys.* **2011**, *13*, 13860−13872.
(20) Del Bene, J. E.; Alkorta, I.; Sánchez-Sanz, G.; Elguero, J. $^{31}P-^{31}P$ Spin−Spin Coupling Constants for Pnicogen Homodimers. *Chem. Phys. Lett.* **2011**, *512*, 184−187.
(21) Del Bene, J. E.; Alkorta, I.; Sánchez-Sanz, G.; Elguero, J. Structures, Energies, Bonding, and NMR Properties of Pnicogen Complexes H_2XP:NXH_2 (X = H, CH_3, NH_2, OH, F, Cl). *J. Phys. Chem. A* **2011**, *115*, 13724−13731.
(22) Adhikari, U.; Scheiner, S. Effects of Carbon Chain Substituents on the P···N Noncovalent Bond. *Chem. Phys. Lett.* **2012**, *536*, 30−33.
(23) Li, Q.-Z.; Li, R.; Liu, X.-F.; Li, W.-Z.; Cheng, J.-B. Pnicogen−Hydride Interaction between FH_2X (X = P and As) and HM (M = ZnH, BeH, MgH, Li, and Na). *J. Phys. Chem. A* **2012**, *116*, 2547−2553.
(24) Li, Q.-Z.; Li, R.; Liu, X.-F.; Li, W.-Z.; Cheng, J.-B. Concerted Interaction between Pnicogen and Halogen Bonds in XCl-FH_2P-NH_3 (X = F, OH, CN, NC, and FCC). *ChemPhysChem.* **2012**, *13*, 1205−1212.
(25) Del Bene, J. E.; Alkorta, I.; Sánchez-Sanz, G.; Elguero, J. Structures, Binding Energies, and Spin−Spin Coupling Constants of Geometric Isomers of Pnicogen Homodimers $(PHFX)_2$, X = F, Cl, CN, CH_3, NC. *J. Phys. Chem. A* **2012**, *116*, 3056−3060.
(26) Del Bene, J. E.; Alkorta, I.; Sánchez-Sanz, G.; Elguero, J. Homo- and Heterochiral Dimers $(PHFX)_2$, X = Cl, CN, CH_3, NC: To What Extent Do They Differ? *Chem. Phys. Lett.* **2012**, *538*, 14−18.
(27) Alkorta, I.; Sánchez-Sanz, G.; Elguero, J.; Del Bene, J. E. Influence of Hydrogen Bonds on the P···P Pnicogen Bond. *J. Chem. Theor. Comp.* **2012**, *8*, 2320−2327.
(28) Del Bene, J. E; Alkorta, I.; Sánchez-Sanz, G.; Elguero, J. Interplay of F−H···F Hydrogen Bonds and P···N Pnicogen Bonds. *J. Phys. Chem. A* **2012**, *116*, 9205.
(29) An, X.-L.; Li, R.; Li, Q.-Z.; Liu, X.-F.; Li, W.-Z.; Cheng, J.-B. Substitution, Cooperative, and Solvent Effects on π Pnicogen Bonds in the FH_2P and FH_2As Complexes. *J. Mol. Model.* **2012**, *18*, 4325−4332.
(30) Bauzá, A.; Quiñonero, D.; Deyà, P. M.; Frontera, A. Pnicogen-π Complexes: Theoretical Study and Biological Implications. *Phys. Chem. Chem. Phys.* **2012**, *14*, 14061−14066.
(31) Alkorta, I.; Sánchez−Sanz, G.; Elguero, J.; Del Bene, J. E. Exploring $(NH_2F)_2$, H_2FP:NFH_2, and $(PH_2F)_2$ Potential Surfaces: Hydrogen Bonds or Pnicogen Bonds? *J. Phys. Chem. A* **2013**, *117*, 183−191.
(32) Sánchez−Sanz, G.; Alkorta, I.; Elguero, J. Intramolecular Pnicogen Interactions in PHF−$(CH_2)_n$−PHF (n = 2−6) Systems. *ChemPhysChem* **2013**, *14*, 1656−1665.
(33) Del Bene, J. E.; Alkorta, I.; Sánchez-Sanz, G.; Elguero, J. Phosphorus as a Simultaneous Electron-Pair Acceptor in Intermolecular P···N Pnicogen Bonds and Electron-Pair Donor to Lewis Acids. *J. Phys. Chem. A* **2013**, *117*, 3133−3141.
(34) Grabowski, S. J.; Alkorta, I.; Elguero, J. Complexes between Dihydrogen and Amine, Phosphine, and Arsine Derivatives. Hydrogen Bond versus Pnictogen Interaction. *J. Phys. Chem. A* **2013**, *117*, 3243−3251.
(35) Alkorta, I.; Elguero, J.; Del Bene, J. E. Pnicogen-Bonded Cyclic Trimers $(PH_2X)_3$ with X = F, Cl, OH, NC, CN, CH_3, H, and BH_2. *J. Phys. Chem. A* **2013**, *117*, 4981−4987.
(36) Murray, J.; Lane, P.; Clark, T.; Riley, K.; Politzer, P. σ-Holes, π-Holes and Electrostatically-Driven Interactions. *J. Mol. Model.* **2012**, *18*, 541−548.
(37) Paulini, R.; Müller, K.; Diederich, F. Orthogonal Multipolar Interactions in Structural Chemistry and Biology. *Angew. Chem., Int. Ed.* **2005**, *44*, 1788−1805.
(38) Pople, J. A.; Binkley, J. S.; Seeger, R. Theoretical Models Incorporating Electron Correlation. *Int. J. Quantum Chem., Quantum Chem. Symp.* **1976**, *10*, 1−19.
(39) Krishnan, R.; Pople, J. A. Approximate Fourth-Order Perturbation Theory of the Electron Correlation Energy. *Int. J. Quantum Chem.* **1978**, *14*, 91−100.
(40) Bartlett, R. J.; Silver, D. M. Many−Body Perturbation Theory Applied to Electron Pair Correlation Energies. I. Closed-Shell First−Row Diatomic Hydrides. *J. Chem. Phys.* **1975**, *62*, 3258−3268.
(41) Bartlett, R. J.; Purvis, G. D. Many−Body Perturbation Theory, Coupled-Pair Many-Electron Theory, and the Importance of Quadruple Excitations for the Correlation Problem. *Int. J. Quantum Chem.* **1978**, *14*, 561−581.
(42) Del Bene, J. E. Proton Affinities of Ammonia, Water, and Hydrogen Fluoride and their Anions: A Quest for the Basis-Set Limit Using the Dunning Augmented Correlation-Consistent Basis Sets. *J. Phys. Chem.* **1993**, *97*, 107−110.
(43) Dunning, T. H. Gaussian Basis Sets for Use in Correlated Molecular Calculations. I. The Atoms Boron through Neon and Hydrogen. *J. Chem. Phys.* **1989**, *90*, 1007−1023.
(44) Woon, D. E.; Dunning, T. H. Gaussian Basis Sets for use in Correlated Molecular Calculations. V. Core−Valence Basis Sets for Boron through Neon. *J. Chem. Phys.* **1995**, *103*, 4572−4585.
(45) Frisch, M. J.; Trucks, G. W.; Schlegel, H. B.; Scuseria, G. E.; Robb, M. A.; Cheeseman, J. R.; Scalmani, G.; Barone, V.; Mennucci, B.; Petersson, G. A.; et al. *Gaussian09*, Revision A.01; Gaussian, Inc.: Wallingford, CT, 2009.
(46) Bader, R. F. W. A Quantum Theory of Molecular Structure and its Applications. *Chem. Rev.* **1991**, *91*, 893−928.
(47) Bader, R. F. W. *Atoms in Molecules, A Quantum Theory*; Oxford University Press: Oxford, U.K., 1990.
(48) Popelier, P. L. A. *Atoms In Molecules. An introduction*; Prentice Hall: Harlow, England, 2000.
(49) Matta, C. F.; Boyd, R. J. *The Quantum Theory of Atoms in Molecules: From Solid State to DNA and Drug Design*; Wiley-VCH: Weinham, 2007.

(50) Silvi, B.; Savin, A. Classification of Chemical Bonds Based on Topological Analysis of Electron Localization Functions. *Nature* **1994**, *371*, 683.
(51) Keith, Todd A. *AIMAll* (Version 11.08.23); TK Gristmill Software: Overland Park, KS, USA, 2011 (aim.tkgristmill.com).
(52) Noury, S.; Krokidis, X.; Fuster, F.; Silvi, B. *TopMod Package*; Universite Pierre et Marie Curie: Paris, 1999.
(53) Rozas, I.; Alkorta, I.; Elguero, J. Behavior of Ylides Containing N, O, and C Atoms as Hydrogen Bond Acceptors. *J. Am. Chem. Soc.* **2000**, *122*, 11154−11161.
(54) Reed, A. E.; Curtiss, L. A.; Weinhold, F. Intermolecular Interactions from a Natural Bond Orbital, Donor-Acceptor Viewpoint. *Chem. Rev.* **1988**, *88*, 899−926.
(55) Glendening, E. D.; Badenhoop, J. K.; Reed, A. E.; Carpenter, J. E.; Bohmann, J. A.; Morales, C. M.; Weinhold, F. *NBO 5.G*; University of Wisconsin: Madison, WI, 2004.
(56) Schmidt, M. W.; Baldridge, K. K.; Boatz, J. A.; Elbert, S. T.; Gordon, M. S.; Jensen, J. H.; Koseki, S.; Matsunaga, N.; Nguyen, K. A.; Su, S. J.; et al. *Gamess*, version 11; Iowa State University: Ames, IA, 2008.
(57) Bulat, F.; Toro-Labbé, A.; Brinck, T.; Murray, J.; Politzer, P. Quantitative Analysis of Molecular Surfaces: Areas, Volumes, Electrostatic Potentials and Average Local Ionization Energies. *J. Mol. Model.* **2010**, *16*, 1679−1693.
(58) Ditchfield, R. Self-Consistent Perturbation Theory of Diamagnetism I. A Gauge-Invariant LCAO Method for NMR Chemical Shifts. *Mol. Phys.* **1974**, *27*, 789−807.
(59) Perera, S. A.; Nooijen, M.; Bartlett, R. J. Electron Correlation Effects on the Theoretical Calculation of Nuclear Magnetic Resonance Spin−Spin Coupling Constants. *J. Chem. Phys.* **1996**, *104*, 3290−3305.
(60) Perera, S. A.; Sekino, H.; Bartlett, R. J. Coupled−Cluster Calculations of Indirect Nuclear Coupling Constants: The Importance of Non−Fermi Contact Contributions. *J. Chem. Phys.* **1994**, *101*, 2186−2196.
(61) Schäfer, A.; Horn, H.; Ahlrichs, R. Fully Optimized Contracted Gaussian Basis Sets for Atoms Li to Kr. *J. Chem. Phys.* **1992**, *97*, 2571−2577.
(62) Stanton, J. F.; Gauss, J.; Watts, J. D.; Nooijen, M.; Oliphant, N.; Perera, S. A.; Szalay, P. S.; Lauderdale, W. J.; Gwaltney, S. R.; Beck, S.; et al. *ACES II*; University of Florida: Gainesville, FL.
(63) Brupbacher-Gatehouses, B. Fourier Transform Microwave Spectroscopic Study of Gas-Phase $ClPO_2$: Molecular Geometry and Electronic Structure Parameter Determinations. *J. Am. Chem. Soc.* **2000**, *122*, 4171−4176.
(64) Solimannejad, M.; Ramezani, V.; Trujillo, C.; Alkorta, I.; Sánchez-Sanz, G.; Elguero, J. Competition and Interplay between σ-Hole and π-Hole Interactions: A Computational Study of 1:1 and 1:2 Complexes of Nitryl Halides (O_2NX) with Ammonia. *J. Phys. Chem. A* **2012**, *116*, 5199−5206.
(65) Linstrom, P. J., Mallard, W. G., Eds. *NIST Chemistry WebBook*; NIST Standard Reference Database Number 69; National Institute of Standards and Technology: Gaithersburg, MD, http://webbook.nist.gov.
(66) Knop, O.; Boyd, R. J.; Choi, S. C. Sulfur-sulfur bond lengths, or can a bond length be estimated from a single parameter? *J. Am. Chem. Soc.* **1988**, *110*, 7299−7301.
(67) Gibbs, G. V.; Hill, F. C.; Boisen, M. B.; Downs, R. T. Power law relationships between bond length, bond strength and electron density distributions. *Phys. Chem. Minerals* **1998**, *25*, 585−590.
(68) Alkorta, I.; Barrios, L.; Rozas, I.; Elguero, J. Comparison of Models to Correlate Electron Density at the Bond Critical Point and Bond Distance. *THEOCHEM* **2000**, *496*, 131−137.
(69) Alkorta, I.; Elguero, J. Fluorine-Fluorine Interactions: A NMR and AIM Analysis. *Struct. Chem.* **2004**, *15*, 117−120.
(70) Tang, T. H.; Deretey, E.; Knak Jensen, S. J.; Csizmadia, I. G. Hydrogen Bonds: Relation Between Lengths and Electron Densities at Bond Critical Points. *Eur. Phys. J. D* **2006**, *37*, 217−222.
(71) Vener, M. V.; Manaev, A. V.; Egorova, A. N.; Tsirelson, V. G. QTAIM Study of Strong H-Bonds with the O−H···A Fragment (A = O, N) in Three-Dimensional Periodical Crystals. *J. Phys. Chem. A* **2007**, *111*, 1155−1162.
(72) Mata, I.; Alkorta, I.; Molins, E.; Espinosa, E. Universal Features of the Electron Density Distribution in Hydrogen-Bonding Regions: A Comprehensive Study Involving H···X (X = H, C, N, O, F, S, Cl, π) Interactions. *Chem. Eur. J.* **2010**, *16*, 2442−2452.
(73) Zeng, Y.; Li, X.; Zhang, X.; Zheng, S.; Meng, L. Insight into the Nature of the Interactions of Furan and Thiophene with Hydrogen Halides and Lithium Halides: Ab Initio and QTAIM Studies. *J. Mol. Model* **2011**, *17*, 2907−2918.
(74) Castillo, N.; Robertson, K. N.; Choi, S. C.; Boyd, R. J.; Knop, O. Bond length and the electron density at the bond critical point: X-X, Z-Z, and C-Z bonds (X = Li-F, Z = Na-Cl). *J. Comput. Chem.* **2008**, *29*, 367−379.
(75) Bader, R. F. W.; Stephens, M. E. Spatial localization of the electronic pair and number distributions in molecules. *J. Am. Chem. Soc.* **1975**, *97*, 7391−7399.